

CHAPTER 4

PROTON TRANSFER IN WATER AND IMIDAZOLE SYSTEMS: DFT STUDY

4.1 Introduction

Water is essential for proton transfer process in Nafion to function as electrolytic polymer. According to higher rate of water evaporation at high temperature, Nafion has a limitation of working temperature range from spectacular reduction of proton conductivity at this condition. Conductivity of this material at high temperature (80 °C) is reduced by more than ten folds relative to that at lower temperature (60 °C) [1-6]. In addition to membrane dehydration, reduction of ionic conductivity, loss of mechanical strength due to softening of polymer backbone, and increased parasitic losses through high fuel permeation at temperatures above 80 °C were observed in Nafion [1,5]. There are several ways to solve these problems e.g. addition of the composite material to protect water molecules at high temperature [4-6], and developing of a new water-free proton conducting membrane [6-13].

Imidazole-based polymer has been developed as water-free proton conducting membrane [6-13]. Imidazole itself can acts as proton solvent and the protonic charge carriers in membranes for fuel cells [6-8]. Many studies indicated that imidazole can increase proton conductivities by structural diffusion involving proton transfer between immobilized heterocycles correlated with structure diffusion Grotthuss-type

mechanism [6,9,10]. This is generally a very complex process requiring the thermally activated accessibility of quite different configurations, such as very short and elongated hydrogen bonds [6,11].

There are number of theoretical studies of proton diffusion in imidazole [13-25]. Fluorinated imidazoles as proton carriers for water-free fuel cell membranes were studied by Deng *et al.* [13] in order to study the poisoning of platinum (Pt) in the imidazole. The imidazole (Im) and trifluoroimidazole (ImF) were optimized the structure, performed MD simulation, and calculated hopping barrier of proton transfer by B3LYP/6-311G**++ method [14-17]. The results showed that the increase of the N-N distance, the activation barrier for proton transfer increased sharply, and at a certain small N-N distance value, the transfer was barrier free. From this regard, the polyimidazole-based should help enhancing proton conductivity from smaller N-N distance.

The rotational potential energy surface (PES) of imidazole, phosphoric acid, and sulfonic acid bearing alkyl molecules were used to indicate the rotation barrier reported by Paddison *et al.* [18]. The torsional barriers of imidazole, phosphoric acid, and sulfonic acid were 3.9, 10.0, and 15.9 kJ.mol⁻¹, respectively. These indicated that the imidazole was clearly the most labile when tethered to an alkyl chain. The binding energy of 2-methyl imidazole and water molecule was lower than that of phosphoric acid and sulfonic acid. From Paddison *et al.* study, imidazole linked with alkyl chain can flexibly move and the water retained in the model showed the imidazole is more hydrophobic than oxo-acids.

To study effect of such fluctuation through the reorientation, Car-Parrinello molecular dynamics (CPMD) simulation which used QM calculation for potential term was employed [13-19]. These previous works suggested that the suitable simulation time and time step should be in ranges of 1-10 ps and 0.1-1 fs respectively. In Münch *et al.* study [19], the imidazole crystal system consisting of two repeating units along *c* axis of imidazole crystal [20] was used for CPMD simulation. They found that the use of simulation time of 6 ps can achieved the configurations of imidazole transition and protonic defect neighborhood in the mechanism. The configuration was found having significant impact on proton transfer. However, they suggested that the simulation time was too short to observe a successful reorientation step.

In the recommendation of Iannuzzi and Parrinello [21], the diffusion process cannot be observed by short span of *ab initio* MD simulation which used *ab initio* calculation for potential term because the process has large energy barriers. For the reason, they developed metadynamics (MTD) technique [21-24], which allows large barriers to be overcome in an affordable simulation time (a few picoseconds). In the research of Iannuzzi *et al.* [21], the proton transfer in heterocyclic crystal was studied by using MTD technique. Note that classical MD simulation and annealing methods were used for system equilibration followed by MTD simulation. The 2x1x3 repeating unit was relaxed by standard MD at 180 K first and by simulated annealing afterwards. Only one unit cell, four molecules per chain with one more proton was selected to calculate charge (Ch) defect and the repulsion between the two close H atoms inducing rotation of neighboring molecule, so called *R* defect.

After MTD simulation, it was able to observe the migration of Ch defect over the four molecules forming the chain in less than 15 ps of simulation time. The result analyzed from MTD trajectory had shown a complex diffusion pathway, moving through similar intermediate states and over barriers of 10-15 kcal.mol⁻¹.

Among numbers of researches focusing on material design of water-free proton conducting material using atomistic simulation, energy profile along with reorientation in electric driving force still, however, mostly excluded. An electric field effect on proton transfer in water system was studied using B3PW91/6-311++G** calculation in gas phase by Li *et al.* [26]. The external electric field in the range of $\pm 5.14 \times 10^6$ to $\pm 10.28 \times 10^7$ V.cm⁻¹ (0.001-0.020 a.u.) were applied in a dimension which aligned in proton transfer path. They found when the electric field was applied in a direction opposite to that of the system dipole, the activation barrier for proton transport was significantly reduced. To include this relevant driving force, the investigation of the electric field effect in water and imidazole by QMMD simulations will be performed in this work prior to the further application in more complicated imidazole-base material design.

4.2.1 Methodology

4.2.1 Directly proton transfer of water and imidazole systems

In this research, hydronium ion (H₃O⁺) and imidazolium ion (ImH⁺) were used for proton donors in water and imidazole systems respectively. The isolated models of water, H₃O⁺, imidazole, and imidazolium ion were built and optimized using BLYP functional

of the generalize gradient approximation (GGA) in DMol3 module of the Material Studio version 5.5 (MS. 5.5) program [27]. The optimized structures were shown in Figure 4.1 (a) and (b). Directly proton transfers in water and imidazole were carried out by scanning potential energy via molecular distance in each couple molecules system. The directly proton transfer system of water consisted of one water molecule and one H_3O^+ . Likewise, two imidazoles system consisted of one imidazole molecule and one imidazolium ion. The initial structure of directly proton transfer study are shown in Figure 4.1 (c). The orientation barriers of water and imidazole systems were dicated by torsional PESs of $\text{H}(\text{H}_3\text{O}^+)-\text{O}(\text{H}_3\text{O}^+)-\text{O}(\text{H}_2\text{O})-\text{H}(\text{H}_2\text{O})$ or Φ and $\text{H}(\text{ImH}^+)-\text{N}(\text{ImH}^+)-\text{N}(\text{Im})-\text{H}(\text{ImH}^+)$ or Ψ respectively. The torsion angles which selected for PES calculation were shown in Figure 4.1 (d).

Additionally, electric field effect on proton transfer was carried out by comparison of PES of the systems which were applied strength electric fields along Z dimension of $\pm 0.0025 (1.29 \times 10^7 \text{ V.cm}^{-1})$, $\pm 0.0050 \text{ a.u. } (2.57 \times 10^7 \text{ V.cm}^{-1})$, and without electric field. The positive and negative applied electric field systems were shown in Figure 4.2(a) and (b) respectively.

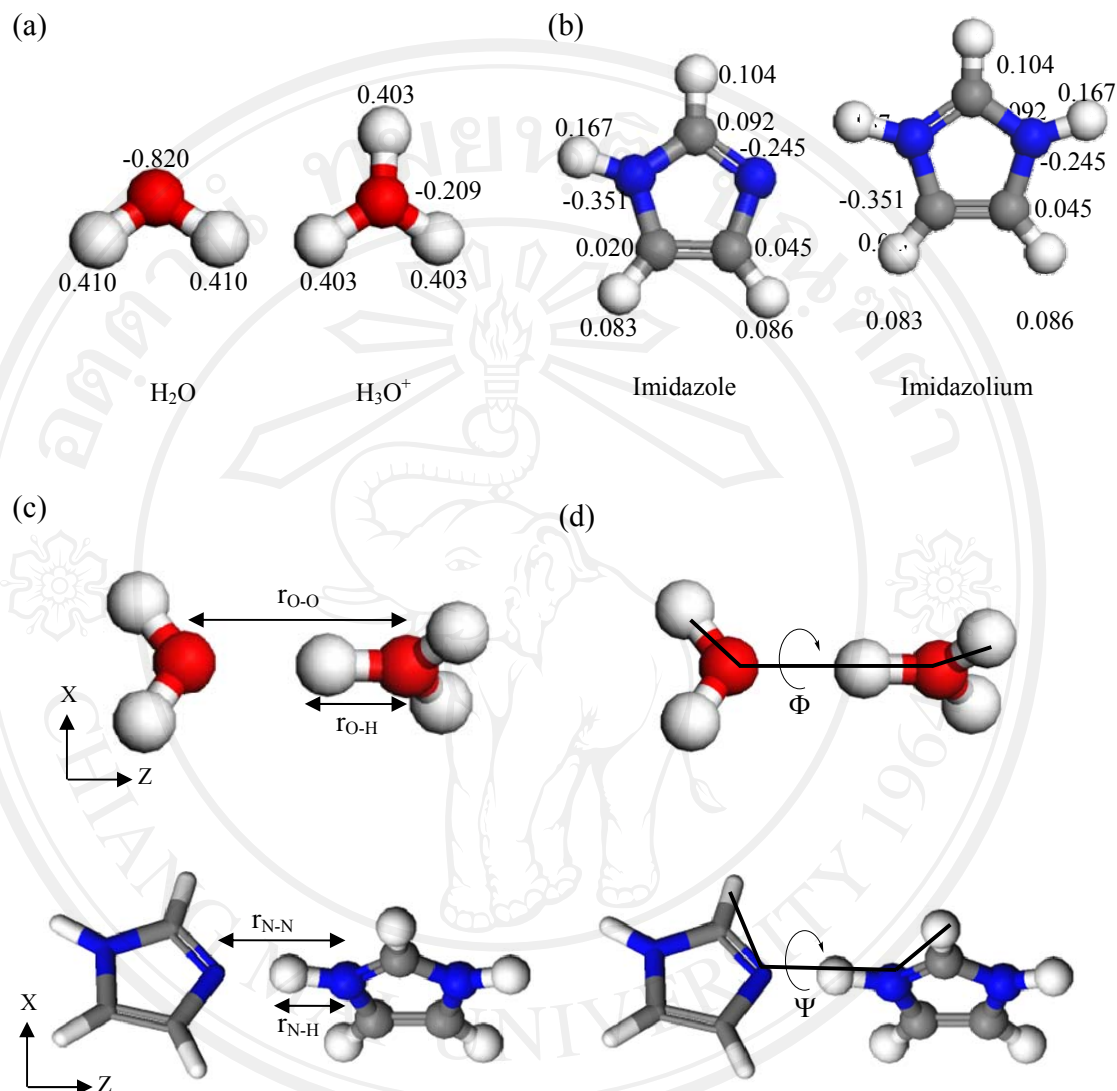


Figure 4.1 Structures of (a) optimized water and H_3O^+ single models with their charges, (b) optimized imidazole and imidazolium ion single models with their charges, (c) initial structure of proton transfer from H_3O^+ to water and imidazolium ion to imidazole, and (d) torsional angle for analysis of rotational barrier of water and imidazole system

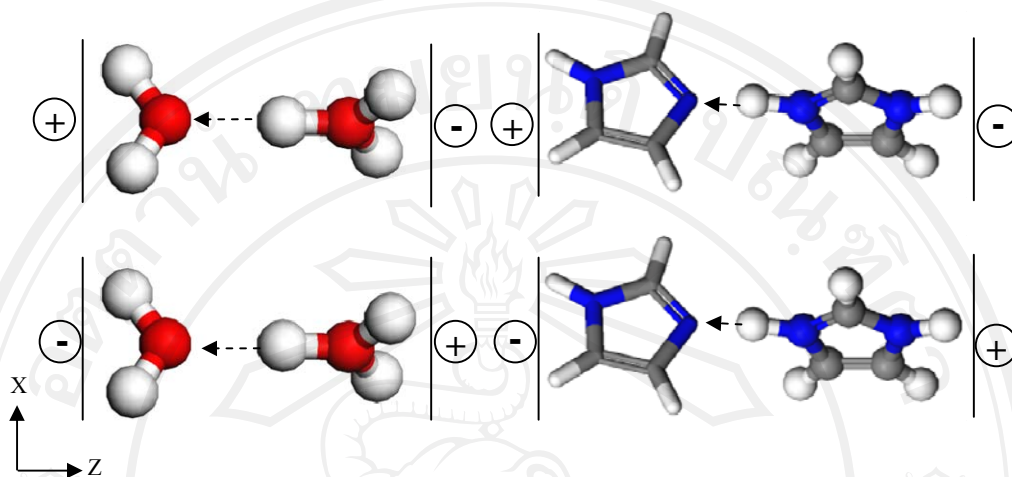


Figure 4.2 Directly proton transfer from H_3O^+ to H_2O (left) and imidazolium ion to imidazole (right) which were applied positive (a) and negative (b) values of electric fields

4.2.2 Periodic models of water and imidazole systems

Model of sixty water molecules and one H_3O^+ in periodic box was constructed by random method of Amorphous Cell module of the Material Studio version 5.5 and COMPASS force field was utilized to calculate interactions of the generated system. The lowest energy structure of ten different energy configurations of this system was chosen for initial structure of further MD simulation. The density was set to 1 g/cm^3 in a box size of $9.00 \times 9.00 \times 22.54 \text{ \AA}^3$. The structural energy of the system was optimized using BLYP functional of GGA approximation in Dmol³ module. The minimized structure of water MD box was shown in Figure 4.3.

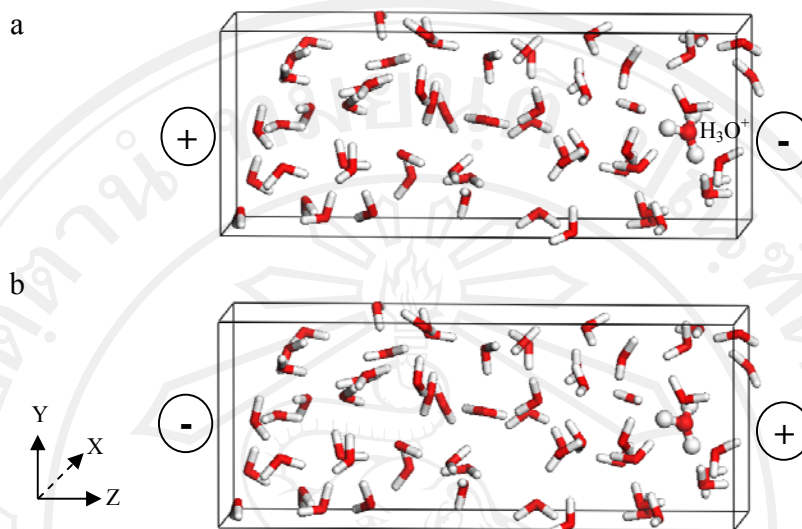


Figure 4.3 Initial structure of water system. (a) and (b) are the systems of positive and negative electric fields which were applied along Z dimension.

The structure of imidazole system was initiated by building of superlattice of imidazole crystal [28] along Z dimension 3 units as shown in Figure 4.4. One hydrogen ion (H^+) was added in the system to form ImH^+ . Before performing of MD simulation, the system was optimized in the same way as performed in the water system.

The optimized model of imidazole prior to MD simulation was shown in Figure 4.4 (b) and (c).

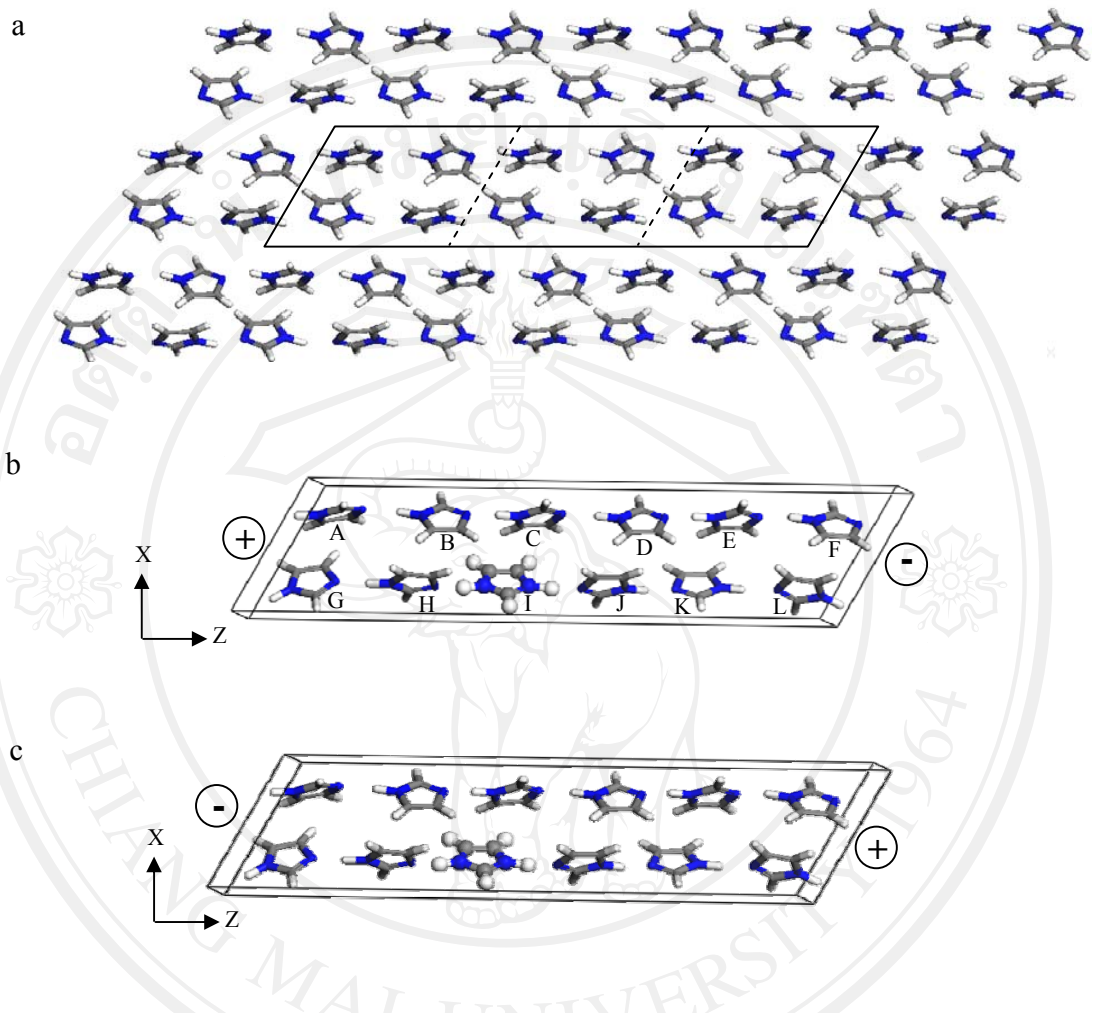


Figure 4.4 Imidazole system: (a) superlattice of imidazole crystal,

(b) imidazole MD box which was applied positive

electric field along Z dimension, and (c) imidazole

MD box which was applied negative electric field along

Z dimension

4.2.3 MD simulations

MD simulation which used DFT calculation for potential term or called DFT-MD simulation was carried out to indicate the molecular interaction such as proton hopping in these systems. BLYP functional of GGA approximation was used for potential energy calculation. NVT ensemble using Nosé-Hoover algorithm, NH chain thermostat [29] for control of temperature was used for both systems. Time step of 1.0 fs was used for simulation until 5.0 ps at temperature of 298 K. Not only simulation of without electric field condition and also applied electric field along Z dimension in the range of -0.0025 until $+0.0050$ a.u. by increasing of 0.0025 a.u. conditions were performed to study the electric field effect. The positive and negative poles of were assigned during apply electric field of each system as shown in Figure 4.3, 4.4 (b) and 4.4 (c).

4.3 Results and discussion

4.3.1 Directly proton transfer from H_3O^+ to H_2O

The effect of molecular distance on proton transfer between water molecules was studied through the change in energy barrier between two water molecules in gas phase as shown in PES plot (Figure 4.5). Variation of distance between oxygen atoms of water molecules ($r_{\text{O-O}}$) was carried out. The results indicate the lowering of the energy barrier of proton transfer increased when $r_{\text{O-O}}$ was decrease and the barrier was found disappear when $r_{\text{O-O}}$ equal to 2.50 Å corresponding to zundel ion (H_5O_2^+) formation.

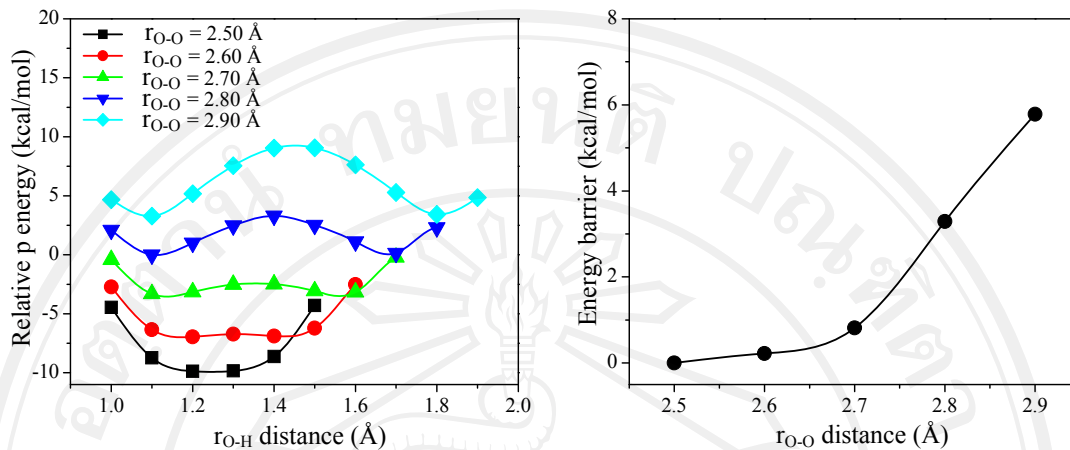


Figure 4.5 Energy barrier of proton hopping between two water molecules; (a) PES at r_{O-O} profile, and (b) relation of energy barrier and molecular distance

At the fixed r_{O-O} at 2.80 Å and structure potential energy as a function of Φ torsion angle with step of 30° was calculated as shown in Figure 4.6. The lowest energy structure was found for twisted couple with Φ of 90° . In comparison of torsional barrier when varied r_{O-O} , lower torsional barrier was found when r_{O-O} was shorter. The result show that with slightly change of inter molecular distance of only 0.40 Å can increase relevant increase of energy barrier almost 1 kcal/mol. This emphasized the hindrance an effect quite importance here so that the possibility those two molecules should move close together then rotate structure in proton transfer processing rather difficult to occur.

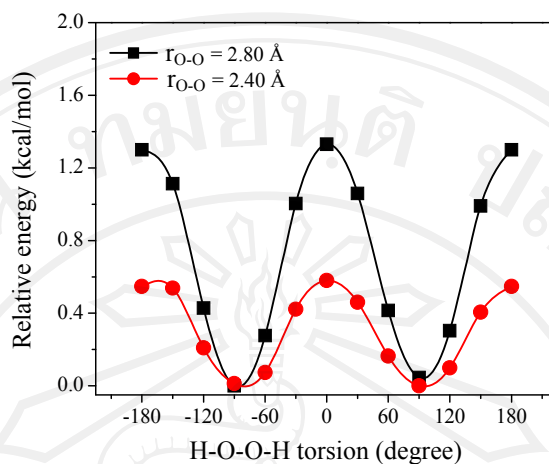


Figure 4.6 Rotational barrier of H_3O^+ and H_2O orientation

When, electric field was applied to investigate effect on proton transfer between two water molecules. The change of energy barrier with r_{O-O} and Φ torsion angle at 2.80 \AA and 90° was investigated. In the model, proton ion was set initially on the right in Figure 4.2 and PES plot as a function of electric field was shown in Figure 4.7. From the calculations, energy barrier of the system gradually decrease under applied electric field from $+0.0050$ to -0.0050 a.u. systematically when applied the electric field in opposite direction (positive value) with proton transfer. It's to say that, the external force in anti parallel direct will retard the hopping but the parallel force will accelerate the movement by increase energy of reactant but stabilize product brought to the change of the profile accomplishing proton hopping.

Interestingly, the effect of field on imidazole is different from applied electric than that of water. In Figure 4.7, the profile indicates the change of reaction coordinates

of transition state in this case and barrier of reaction totally disappear at electric field of -0.0050 a.u.

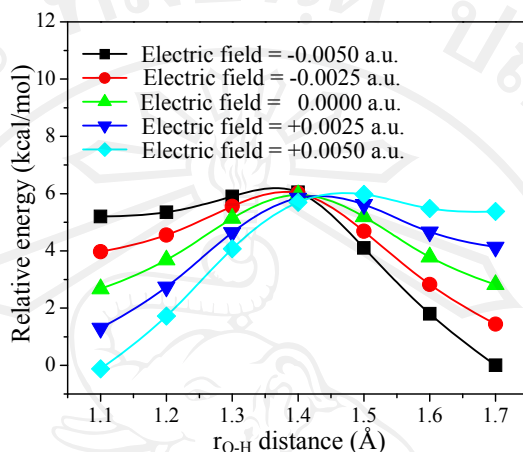


Figure 4.7 Electric field effect on proton hopping from H_3O^+ to H_2O

4.3.2 Dynamics properties of proton transfer in water system

The study was extended in order to include effect of long length interactions which is important in liquid state. Proton hopping in water system was observed from DFT-MD simulations. The movements of proton hopping in the systems under applied electric field of -0.0050 a.u. and +0.0050 a.u. were shown in Figure 4.8 and 4.9 respectively. The trajectory plots of H1 (see H1 position in Figure 4.8) confirmed that the electric field can control proton movement direction. In the positive applied electric field system (Figure 4.10 (a)), the positive slope of trajectory plot was found. In the other hand, the negative slope of trajectory plot was observed in negative applied electric field system.

The proton diffusion coefficient was used to examine the efficiency of proton conduction. The diffusion coefficient can be calculated by the Einstein diffusion equation [5,27,30] from Chapter 1. The averaged diffusion coefficients of hopping H atoms of -0.0025 , -0.0050 a.u., and without electric field were shown in Table 4.1. The movements of three hydrogen atoms which hopped stepwise in each system were sampling for proton diffusion coefficient calculation. Whereas, two sequential steps of proton transfer were found in the system of without electric field applying. The calculated result was validated with experimental observation, diffusion coefficient calculated from DFT-MD simulations was found of $0.176 \text{ \AA}^2 \cdot \text{ps}^{-1}$ which is lower than experimental value only $0.054 \text{ \AA}^2 \cdot \text{ps}^{-1}$.

The increasing of averaged diffusion coefficient was found when the electric field was increased in magnitude from -0.0025 a.u. to -0.0050 a.u.. The values of both applied electric fields are higher than that without electric field. The simulations confirm that the systems with applied electric field have better proton transfer efficiency than without.

Table 4.1 Proton diffusion coefficient of water system

Electric field (a.u.)	Average diffusion coefficient $D = \frac{1\langle(r_t - r_0)^2\rangle}{6\Delta t}$ (Å ² .ps ⁻¹)
0.0000	0.176
-0.0025	2.452
-0.0050	3.513
Experiment ^[31]	0.230

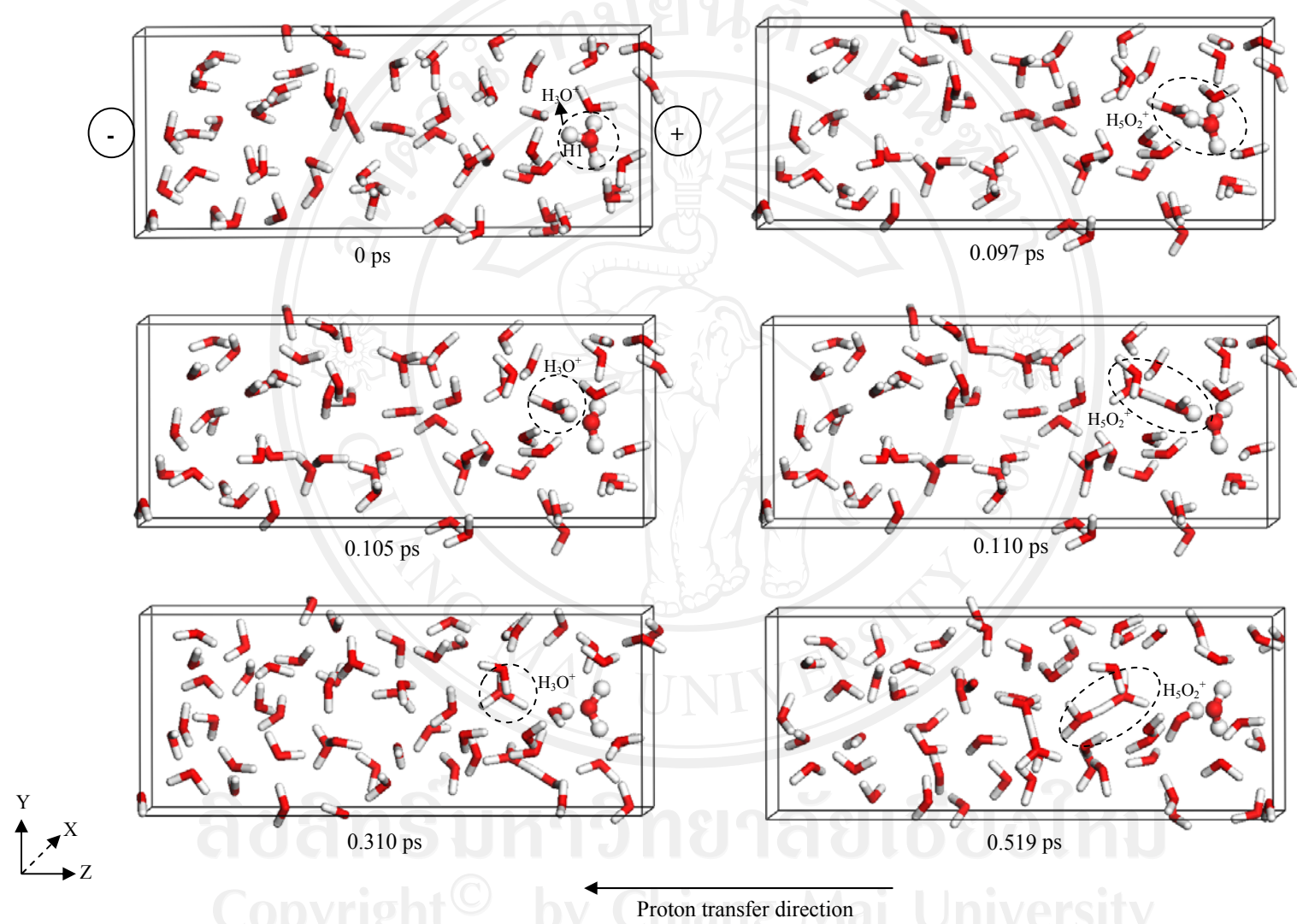


Figure 4.8 Snapshot of proton transfer in water system which was applied -0.0050 a.u.

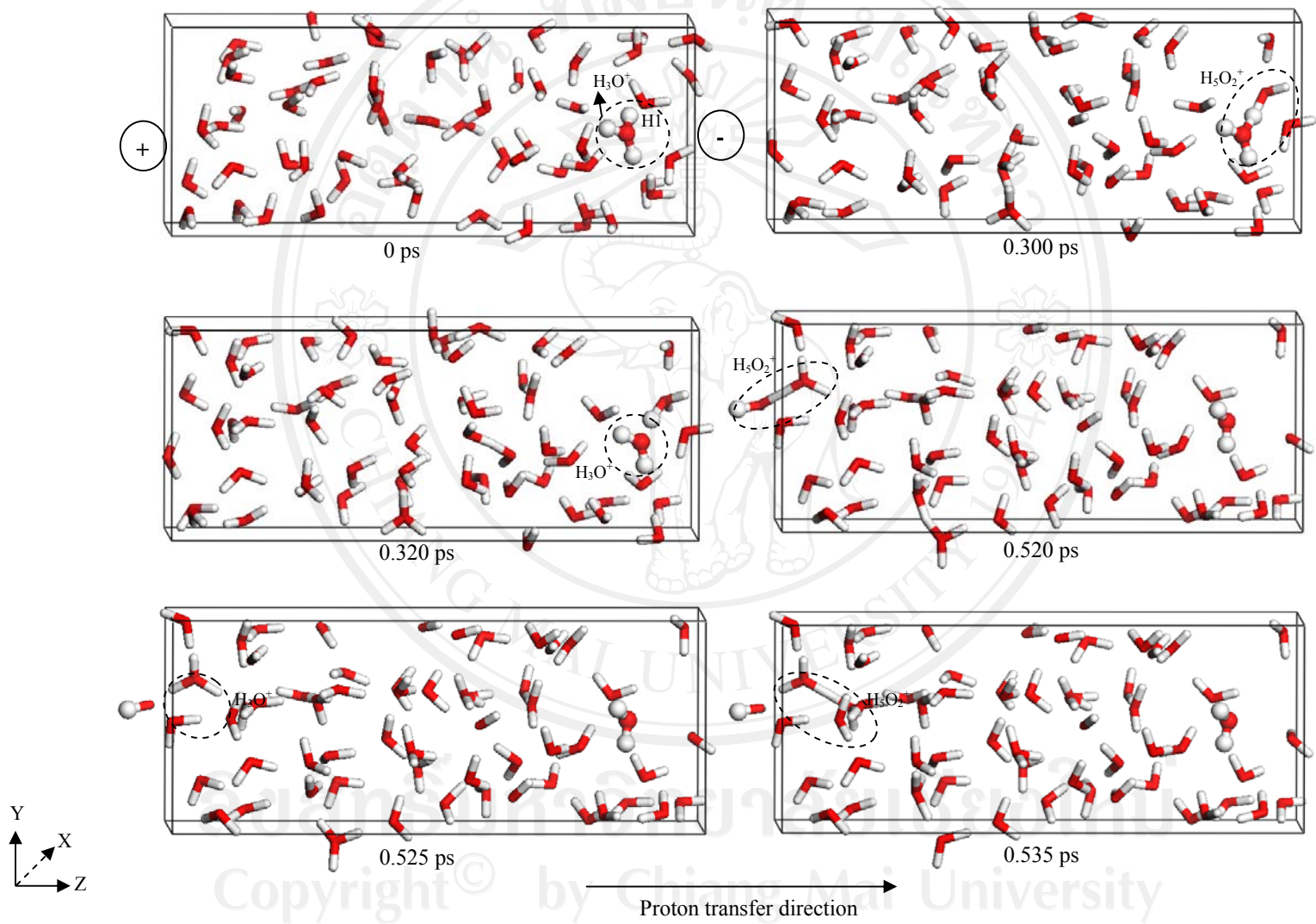


Figure 4.9 Snapshot of proton transfer in water system which was applied +0.0050 a.u.

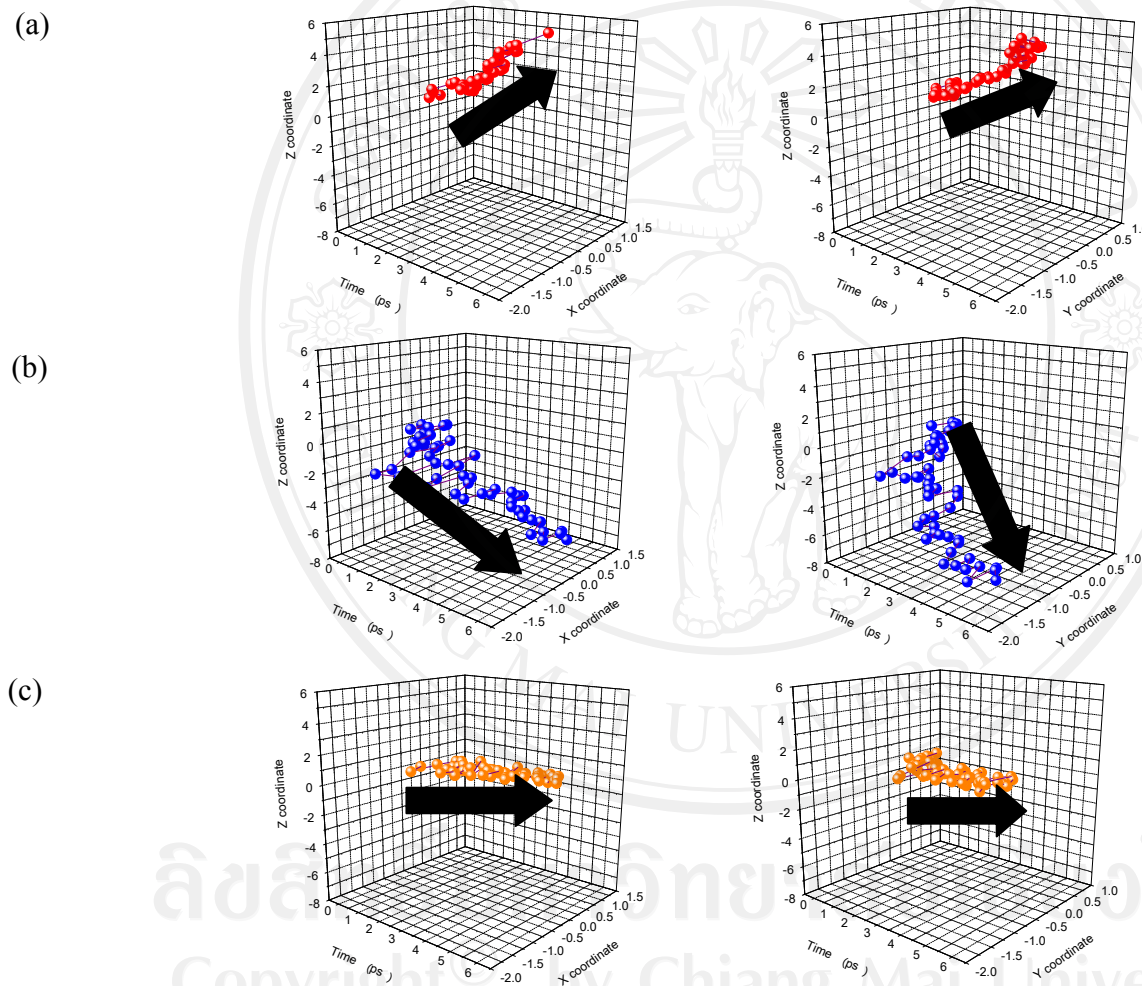


Figure 4.10 Trajectory plots of H1 along XZ and YZ planes. (a) applied electric field = +0.0050 a.u., (b) applied electric field = -0.0050 a.u., and (c) without electric field



ลิขสิทธิ์มหาวิทยาลัยเชียงใหม่

Copyright© by Chiang Mai University

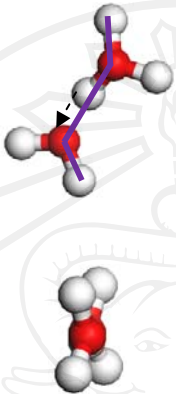
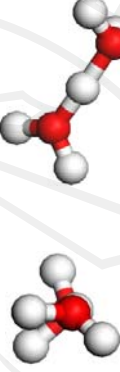
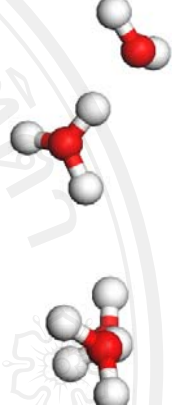
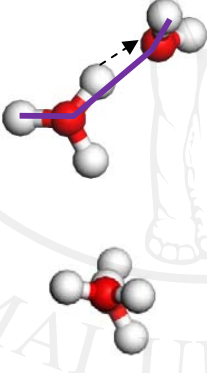
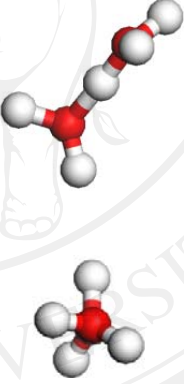
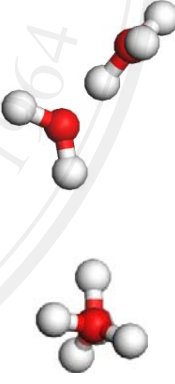
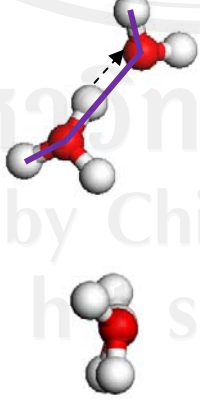
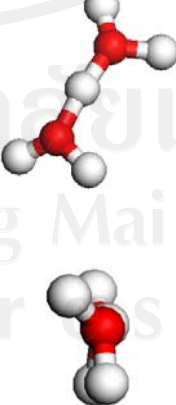
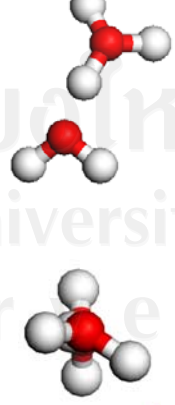
All rights reserved

4.3.4 Molecular orientation of water system during proton transfer

The direction of proton transfer depended on electric field value. The proton transfer from original position along Z dimension when electric field was applied in positive value as shown the snapshots of -0.0050 a.u. applied electric field in Figure 4.10. In the other hand, the proton transferred opposite direction of Z dimension when applied electric field in positive value as shown the snapshots of +0.0050 a.u. in Figure 4.11. Trajectory of proton movement monument water molecule in virtual box was projected as a function of time in Figure 4.10. In the proton transfer direction of +0.0050 a.u., the plot of XZ and YZ coordinates during simulation time in Figure 4.12 (a) shown the positive slope of both graphs whereas the negative slopes of -0.0050 a.u. from Figure 4.12 (b) were found. Without electric field, the slopes of Z change were likely to near zero.

The rotational of water during proton transfer was observed. In the proton transfer process of water system, H_3O^+ was formed at first, and move then near to the another water as zundel ion (H_5O_2^+) or eigen ion (H_7O_3^+), and the proton was transferred from donor to acceptor water molecules at the final step. In this simulation, the donor and acceptor structures of 3 steps of H1 transfer process were snapped to analysis the structural rotation. The rotational of water system was examined by measurement of Φ torsion angle of donor to acceptor water molecules as shown in Table 4.2 which is similar to two water molecules in gas phase case.

Table 4.2 Orientation of H_3O^+ and H_2O during proton transfer process

Electric field (a.u.)	Initial structure	Zundel formation	After proton hopping
0	 Torsion = 58.063°	 Torsion = -149.014°	 Torsion = -168.972°
-0.0025	 Torsion = 88.23°	 Torsion = 83.74°	 Torsion = 78.92°
-0.0050	 Torsion = 37.902°	 Torsion = 33.245°	 Torsion = 88.232°

However, the initial structures were different conformations (gauche and straggled), almost of structures were like change to be straggled conformation or trans conformation because of repulsion force. This phenomenon was supported by the section 4.2.1. Therefore, proton hopping, rotational of structure, controlling of proton transfer direction by electric field value, were found by QMMD simulations of water system.

4.3.5 Directly proton transfer from imidazolium to imidazole

Energy change during proton transfer process between two imidazoles was performed as described in precious section. Effect of inter molecular distance was carried out by PES in term of distance between nitrogen atoms (r_{N-N}) (Figure 4.7). Potential energy profiles of H moving from NH to N were found change from profile with high barrier (15 kcal/mol) of $N-N = 3.00 \text{ \AA}$ to without barrier of 2.50 \AA [13]. In rotational effect, the opposite orientation of two imidazoles was found at lowest barrier which can be overcome at room temperature as shown in Figure 4.8. Threshold of barrier change was found of r_{N-N} of 2.70 \AA as shown in Figure 4.7 (b).

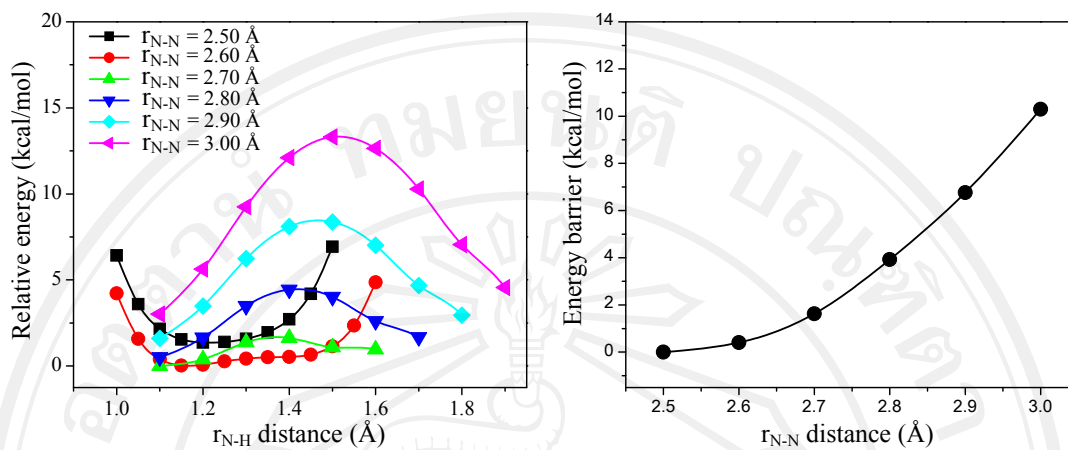


Figure 4.11 Energy barrier of proton hopping between two imidazoles;

(a) PES when varied r_{N-N} , and (b) relationship of energy barrier and r_{N-N}

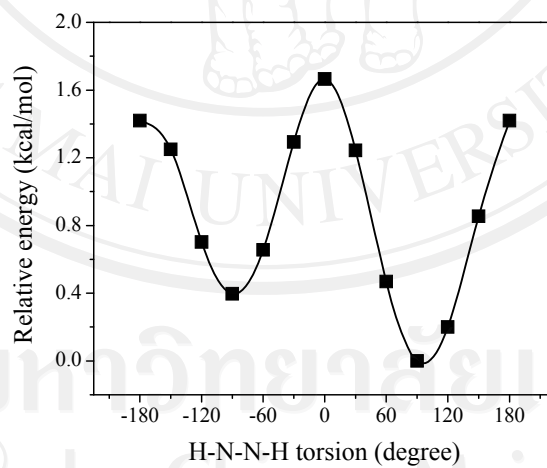


Figure 4.12 Rotational barrier of proton transfer between two imidazoles

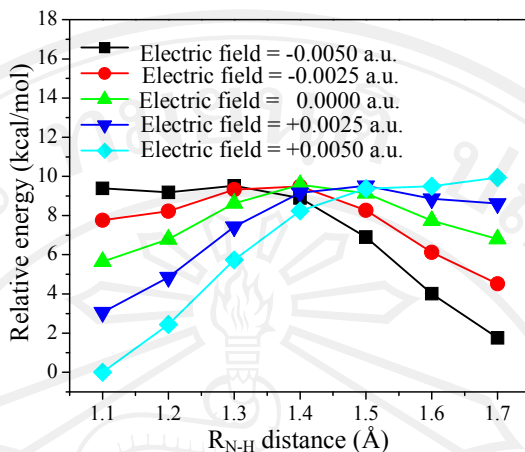


Figure 4.13 Electric field effect on proton hopping between two imidazoles

4.3.6 Dynamics properties of proton transfer in imidazole

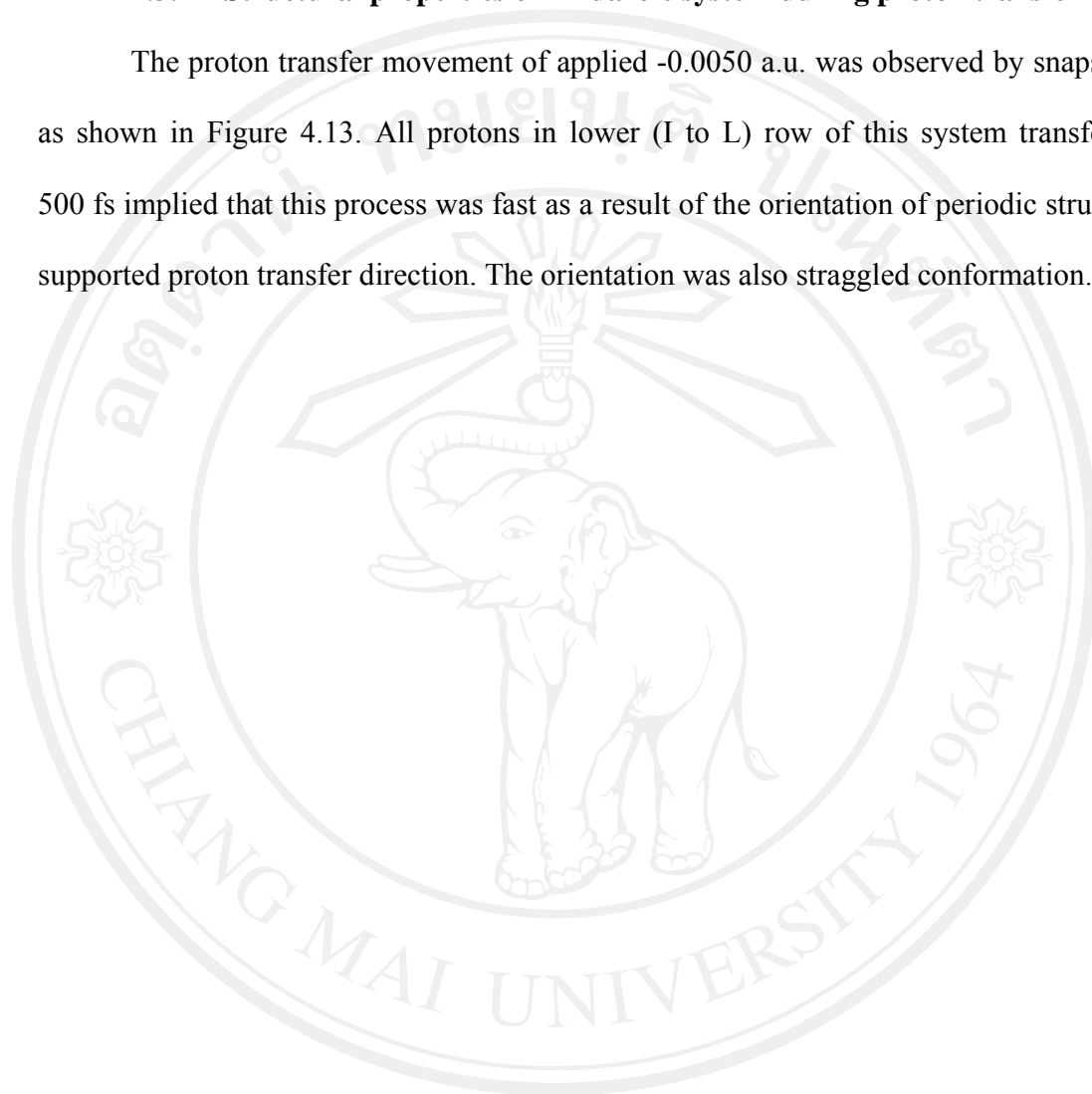
The proton transfer of imidazole case was calculated as described in periodic system. The proton diffusion coefficients of without, applied -0.0050 a.u., and -0.0075 a.u. electric fields were shown in Table 4.3. Increasing of diffusion coefficient was observed when the electric field was increased.

Table 4.3 Proton diffusion coefficient of imidazole system

Electric field (a.u.)	Average diffusion coefficient $D = \frac{1((r_t - r_0))^2}{6\Delta t}$ (Å ² .ps ⁻¹)
0.0000	0.106
-0.0050	2.123
-0.0075	2.520

4.3.7 Structural properties of imidazole system during proton transfer

The proton transfer movement of applied -0.0050 a.u. was observed by snapshots as shown in Figure 4.13. All protons in lower (I to L) row of this system transferred 500 fs implied that this process was fast as a result of the orientation of periodic structure supported proton transfer direction. The orientation was also straggled conformation.



ลิขสิทธิ์มหาวิทยาลัยเชียงใหม่
Copyright© by Chiang Mai University
All rights reserved

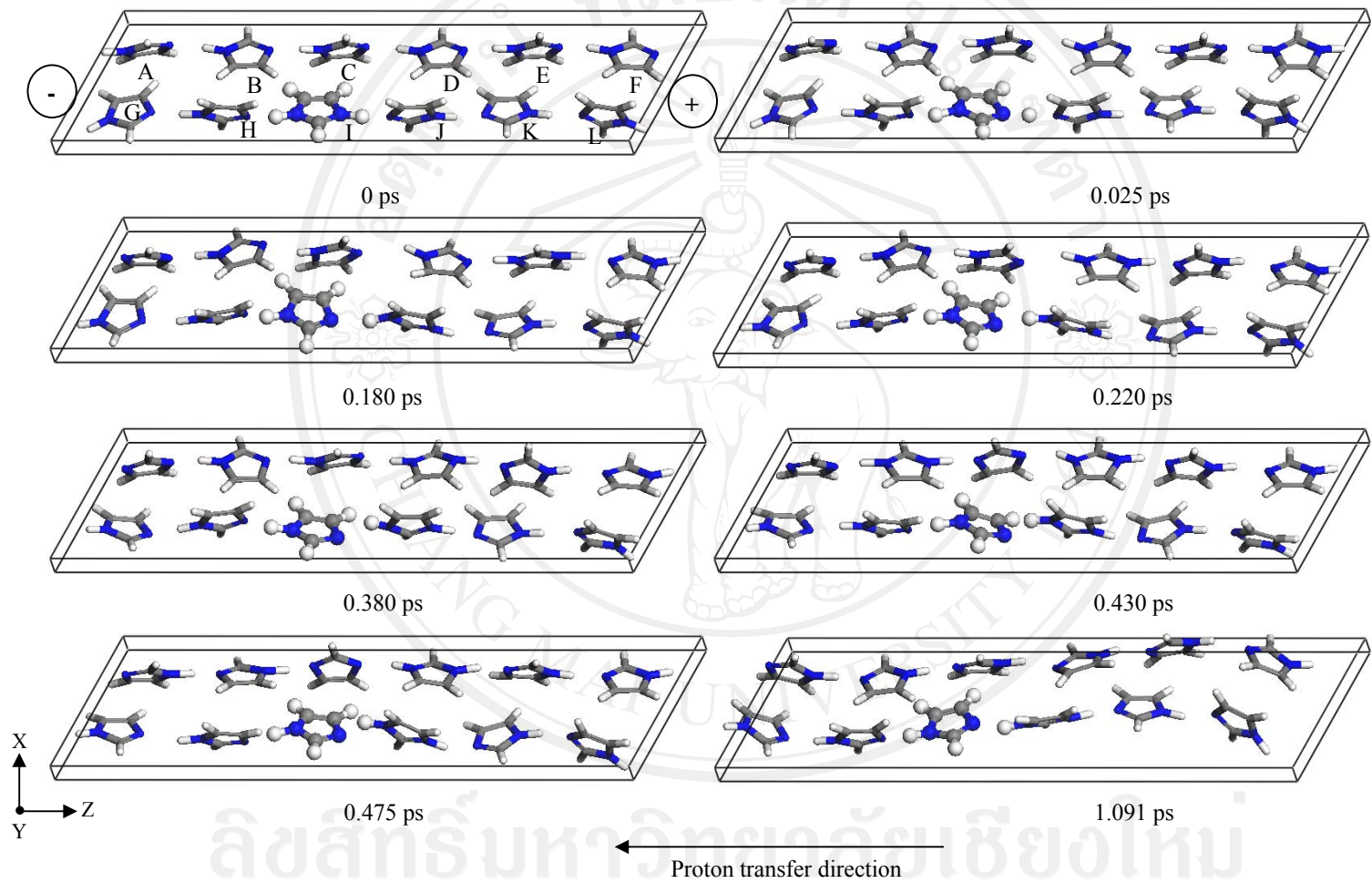


Figure 4.14 Snapshot of directly proton transfer in imidazole system which was applied -0.0050 a.u.

4.4 Conclusion

The DFT calculations of directly proton transfer from H_3O^+ to H_2O and imidazolium ion to imidazole cases can describe the energy barrier of proton hopping and molecular orientation. The barrier indicated the easily of proton transfer of structural rotation. The molecular distance, structural orientation, and electric field have effect on proton transfer barrier. The shorter molecular distance, trans orientation, and higher electric field which support in the proton transfer direction, have better proton diffusion efficiency. In many molecules, the proton hopping process and phenomena during proton transfer of both systems were observed by DFT-MD simulations. The electric field also affected on proton diffusion efficiency.

References

- [1] Smitha, B.; Sridhar, S.; Khan, A. A. *Journal of Membrane Science* **2005**, 259, 10-26.
- [2] Costamagna, P.; Srinivasan, S. *Journal of Power Sources* **2001**, 102, 242–252.
- [3] Rikukawa, M.; Sanui, K. *Progress in Polymer Science* **2000**, 25, 1463–1502.
- [4] Gosalawit, R.; Chirachanchai, S.; Manuspiya, H.; Traversa, E. *Catalysis Today* **2006**, 118, 259-265.
- [5] Yana, J.; Nimmanpipug, P.; Chirachanchai, S.; Gosalawit, R.; Dokmaisrijan, S.; Vannarat, S.; Vilaithong, T.; Lee, V.S. *Polymer* **2010**, 51, 4632-4638.
- [6] Schuster, M.; Meyer, W. H.; Wegner, G.; Herz, H. G.; Ise, M.; Schuster, M.; Kreuer, K. D.; Maier, J. *Solid State Ionics* **2001**, 145, 85-92.

- [7] Kreuer, K.D.; Fuchs, A.; Ise, M.; Spaeth, M.; Maier, J. *Electrochim. Acta* **1998**, *43*, 1281-1288.
- [8] Kreuer, K.D. *Solid State Ionics* **1997**, *97*, 1-15.
- [9] Kreuer, K.D. *Solid State Ionics* **1997**, *94*, 55-62.
- [10] Agmon, N. *Chem. Phys. Lett.* **1995**, *244*, 456.
- [11] Kreuer, K. D.; Adams, St.; Münch, W.; Fuchs, A.; Klock, U.; Maier, J. *Solid State Ionics* **2001**, *145*, 295-306.
- [12] Pangon, A.; Totsatitpaisan, P.; Eiamlamai, P.; Hasegawa, K.; Yamasaki, M.; Tashiro, K.; Chirachanchai, S. *Journal of Power Sources* **2011**, *196*, 6144-6152.
- [13] Deng, W.Q.; Molinero, V.; Goddard, W.A. *Journal of the American Chemical Society* **2004**, *126*, 15644-15645.
- [14] Winget, P.; Clark, T.; *Journal of Computational Chemistry* **2004**, *25*, 725-733.
- [15] Becke, A. D. *Journal of Chemical Physics* **1993**, *98*, 1372-1377.
- [16] Becke, A. D. *Journal of Chemical Physics* **1993**, *98*, 5648-5652.
- [17] Becke, A. D. *Journal of Chemical Physics* **1992**, *97*, 9173-9177.
- [18] Paddison, S.J.; Kreuer, K.D.; Maier, J. *Physical Chemistry Chemical Physics* **2006**, *8*, 4530-4542.
- [19] Münch, W.; Kreuer, K.D.; Silvestri, W.; Maier, J.; Seifert, G. *Solid State Ionics*, **2001**, *145*, 437-443.
- [20] Will, G.Z. *Kristallografiya* **1969**, *129*, 211-221.
- [21] Iannuzzi, M.; Parrinello, M. *Physical Review Letters* **2004**, *93*, 025901-1-025901-4.

- [22] Laio, A.; Parrinello, M. *Proceedings of the National Academy of Sciences of the United States of America* **2002**, *20*, 562.
- [23] Iannuzzi, M.; Laio, A.; Parrinello, M. *Physical Review Letters* **2003**, *90*, 238302-238302.
- [24] Iannuzzi, N. *Journal of Chemical Physics* **2006**, *124*, 204710-1–204710-10.
- [25] Lee, C.T.; Yang W.T.; Parr, R.G. *Physical Review B* **1988**, *37*, 785-789.
- [26] Li, T.; Wlaschin, A.; Balbuena, P.B. *Industrial & Engineering Chemistry Research* **2001**, *40*, 4789-4800
- [27] Materials Studio, Accelrys Software Inc., San Diego, CA, 5.5 edn., **2011**.
- [28] Goddard, R.; Heinemann, O.; Kruger, C., *Acta Crystallographica Section C* **1997**, *53*, 1846-1850.
- [29] Tuckerman, M.E.; Liu, Y.; Ciccotti, G.; Martyna, G.J. *Journal of Chemical Physics* **2001**, *115*, 1678-1702.
- [30] Allen, M.P.; Tildesley, D.J. “Computer Simulation of Liquids” Oxford University Press: Oxford, U.K., **1990**.
- [31] Glättli, A.; Daura, X.; Van Gunsteren, W F. *Journal of Computational Chemistry* **2003**, *24*, 1087-1096.